10.1177/0003702818788828

Design of First-Order 121.6 nm Minus Filters

Xiaodong Wang*[,1], Bo Chen[1], Tonglin Huo[2], Hongjun Zhou[2]

1. State Key Laboratory of Applied Optics, Changchun Institute of Optics, Fine Mechanics and Physics, Chinese Academy of Sciences, Changchun 130033, China

2. National Synchrotron Radiation Laboratory, University of Science and Technology of China, Hefei 230026, China

*wangxiaodong@ciomp.ac.cn

Abstract

The equivalent parameters function in Macleod software can be used to calculate equivalent admittance and phase thickness of multilayer, even though material is absorbing, dispersive, and the incidence angle is not zero. We utilized this software to design first-order 121.6 nm minus filters based on a lanthanum trifluoride (LaF_3)/magnesium fluoride (MgF_2) multilayer; a Gaussian-type target curve was also introduced into the design. Minus filters with bandwidths of 10 nm and 5 nm were obtained, and had good visible light suppression and low sidelobe ripples. This designed filter will be fabricated for utilizing in Lyman-alpha coronagraph and imager installed in Lyman-alpha solar telescope, which will be launched by China in 2021.

Keywords: Minus filter, narrowband, equivalent parameters function, lathanum trifluoride, LaF_3, magnesium fluoride, MgF_2

~~<AQ>This paper was heavily edited for grammar and syntax. Please check carefully.</AQ>~~

Introduction

The Lyman-alpha emission line of hydrogen is 121.6 nm, and it is the imaging target of many solar detection tasks due to its outstanding characteristics.[1–5] A narrowband reflective filter was often utilized in solar observation. There are many other far ultraviolet (UV) emission lines and visible light in solar spectrum; thus, in order to maintain spectral purity of detection, this filter must have low sidelobe ripples and low reflectance in the visible waveband. Reflective narrowband coatings are also called notch mirrors or minus filters. Rodriguez prepared a lanthanum trifluoride (LaF_3)/magnesium fluoride (MgF_2) multilayer with a highest reflectance of 62.7% and a bandwidth of 13.2 nm at 121.6 nm after 12 months of aging.[6] The Al/MgF_2/Os

multilayer was deposited by the Acton Research Company, and this multilayer has a peak reflectance of 51% at 121.6 nm, and a bandwidth of 15 nm.[7] Park designed and fabricated 121.6 nm reflective filters, and two LaF_3/MgF_2 mirrors provided a reflectance of 27% and a bandwidth of 6 nm.[8] The Acton Research Company also provided narrowband coatings with a peak reflectance of higher than 55% at 121.6 nm and a bandwidth of about 7 nm, but the employed materials were not given.[9] According to our literature survey, the sidelobe ripples of previous deposited filters are still too significant. Our group designed second and third order 121.6 nm minus filters with low sidelobe ripples, but they each have another reflectance zone at 203 nm and 280 nm.[10,11] In 2021, China will launch Lyman-alpha Solar Telescope, on which a Lyman-alpha coronagraph and imager are to be installed. A 121.6 nm narrowband reflective filter is urgently demanded in the Lyman-alpha coronagraph and imager.

In this paper, 121.6 nm minus filters with bandwidths of 5 nm and 10 nm were designed, and the sidelobe ripples were suppressed. The equivalent parameters function in Macleod software[12] and a Gaussian-type target curve were utilized in our design.

Design

Minus Filter with a Bandwidth of 10 nm

Used in our design were LaF_3 (H) and MgF_2 (L); H and L denote high- and low-index material, respectively. The substrate is fused silica with a thickness of 1.5 mm. Optical constants of LaF_3 and MgF_2 in 115–760 nm are shown in Figure 1 in the work of Wang and Chen.[11] Optical constants were derived from the characterization of reflectance (10 and 20°) and transmittance (0°) of a single layer with a physical thickness of about 200 nm. Optical performances of films in 115–130 nm were measured by the National Synchrotron Radiation Laboratory, 131–80 nm using a McPherson VUVaS 2000, and 381 – 760 nm using a Lambda 1050 ultraviolet–visible–near-infrared spectrophotometer.

The bandwidth of multilayers can be tuned by adjusting the optical thickness ratio of H/L, and this ratio cannot be too high and too low due to the small thickness limit of 10 nm. In addition, MgF_2 always has a larger stress,[13] thus the fraction of MgF_2 should be lower. Finally, we chose a ratio of 1.4 H/0.6 L. The structure of initial periodic multilayer was sub/(0.7H0.6L0.7H)^11/air, and the incident angle was 10°. Backside reflectance of the substrate was not taken into calculation. The theoretical reflectance curve is shown in the Supplemental

Material Figure S1. ~~<AQ> It is not journal format to list Supplemental Material as a reference item. This reference has been removed from the list and all subsequent references renumbered. Please check all in-text references to ensure the references have been renumbered correctly.</AQ>~~ As shown in Figure S1, the reflectance at 121.6 nm is 76%, the bandwidth is 12 nm, and left side ripples are too significant and need to be further reduced.

The oscillations in the passbands of the stopband result from an index mismatch between multilayer and substrate or air. Thus, the equivalent parameters of the multilayers, equivalent admittance and equivalent phase thickness, need to be calculated. In the far-UV waveband, materials are dispersive and absorbing; therefore, the calculation of equivalent parameters is complicated. Only the equivalent parameters function in Macleod software can perform this calculation. In this function, the product matrix of any combination of layers could be considered into Eq. 1 of the inhomogeneous film matrix. Equivalent parameters of multilayers are regarded as those of a single inhomogeneous layer; E_i and E_o are inner and outer admittance of this layer, respectively, γ is the equivalent phase thickness, which is described by $\delta - i\beta$. When the multilayer is symmetrical, E_i and E_o are equal.[14]

$$\begin{bmatrix} m_{11} & m_{12} \\ m_{21} & m_{22} \end{bmatrix} = \begin{bmatrix} \left(\frac{E_i}{E_0}\right)^{\frac{1}{2}} \cos g & \frac{i \sin g}{\left(E_0 E_i\right)^{\frac{1}{2}}} \\ i\left(E_0 E_i\right)^{\frac{1}{2}} \sin g & \left(\frac{E_i}{E_0}\right)^{\frac{1}{2}} \cos g \end{bmatrix} \quad (1)$$

When the multilayer is illuminated at an oblique incidence, the equivalent parameters function in Macleod software can provide the *p*- and *s*-polarization of the equivalent admittance, respectively. Since $\eta_{p=}y/\cos\theta$ and $\eta_{s=}\ y\cos\theta$, the *p*-polarization of equivalent admittance is slightly bigger than *s*-polarization at an incidence angle of 10°. In this paper, only *p*-polarization of the equivalent admittance is taken into account in the matching discussion because *p*- and *s*-polarizations reveal similar results. It should be noted that refractive index N and optical admittance *y* are numerically equal at optical frequencies by expressing *y* in free space units.[14]

Next, we eliminated the sidelobe ripples of the reflection zone from two cases, the first to match index of multilayer to the air, the second to match the index of the multilayer to the substrate.

Index Matching of Multilayer to Air.

The equivalent parameters function in Macleod software was used to calculate the equivalent parameters of the initial periodic multilayer (see results in Figure S2) and the imaginary part was ignored. The calculated equivalent admittance of the periodic multilayer was 5.04 at 115 nm; the refractive index of the needed antireflection coating between air and the multilayer should be $(5.04\times1)^{0.5}=2.24$, while the refractive index of LaF_3 should be 2.20. Thus, we first utilized the LaF_3 single layer to reduce the mismatch between the air and the periodic multilayer. Figure 1 demonstrates the theoretical reflectance curves of a modified multilayer ((0.7H0.6L0.7H)^11 mH). When the optical thickness of the added LaF_3 single layer is 0.95H (1/4λ at 115 nm), it was found that reflectance at 115 nm was reduced from 10.9% to 2.3%, while the right side ripples of the 121.6 nm stopband became worse. Using the trial and error method, a value of 0.6 for *m* was selected, which resulted in a relatively better spectral response. This designed filter had a reflectance of 83.4% at 121.6 nm and a bandwidth of 12 nm. However, the sidelobe ripples still needed further suppression.

<Insert Fig. 1>

It can be seen in Figure S2 that the equivalent admittance profile far from the edges is flat, while the equivalent admittance near the edges of the stopband has a rapid variance, which makes match index of the multilayer to the substrate or surrounding media complicated. We employ Thelen's shifted equivalent layers (SELs) method to further reduce oscillations near the edge of reflection zone.[14,15] SEL is similar to main multilayer, but has a slightly different thickness. Thus, SEL corresponds to a deviated central wavelength, and it is a commonly targeted wavelength at which mismatch between multilayer and substrate or air needs to be reduced. The period number of SEL should be carefully selected to meet the phase condition of antireflection, that is, the phase thickness of SEL at a matched point should be odd times of quarter-waves. Here, main multilayer is (0.7H0.6L0.7H)^11, SEL is n(0.7H0.6L0.7H). It is found that when *n* is selected to be 0.964, equivalent admittance is 2.248 at 115 nm, which fulfills the admittance condition of anti-reflection. Figure S3 demonstrates the real part of

equivalent admittance of the periodic multilayer 0.964(0.7H0.6L0.7H), and the imaginary part was ignored. Although the phase thickness of the SEL is (1.018–i0.161)π, it is found that when the SEL period is two, the spectral performance is better. Figure 2 shows the theoretical reflectance curve of a multilayer with a structure of sub/((0.7H0.6L0.7H)^9 0.6H0.964(0.7H0.6L0.7H)^2)/air. Comparing Figure 2 with Figure 1, although the reflectance of this designed filter decreases from 83.4% to 70.5% at 121.6 nm, the bandwidth decreases from 12 nm to 10 nm. More importantly, sidelobe ripples are significantly suppressed by the insertion of SEL between multilayer and air. It should be noted that in our design strategy, suppression of sidelobe ripples is more important than peak reflectance.

<Insert Fig. 2>

Index Matching of Multilayer to Substrate

The SEL method was utilized to match the multilayer index to the substrate at 132 nm. It was found that the real part of the equivalent admittance of 0.83(0.7H0.6L0.7H) at 132 nm was 1.637, and it was close to the square root of the product of admittance of the main multilayer (1.314) and fused silica (2.041) ($(1.314\times2.041)^{0.5}$=1.638). In other words, SEL 0.83(0.7H0.6L0.7H) meets the admittance condition of antireflection. However, the physical thickness of each layer in this SEL is less than 10 nm. Thus, SEL 0.9(0.7H0.6L0.7H) was selected, and its equivalent admittance was 1.55 at 132 nm. Figure 3 shows a real part of the equivalent admittance of the multilayer 0.9(0.7H0.6L0.7H). It was also found that when the period selected is two, the spectral response is better. Figure 4 demonstrates the theoretical reflectance curve of the multilayer with a structure of sub/(0.9(0.7H0.6L0.7H)^2 (0.7H0.6L0.7H)^7 0.6H0.964(0.7H0.6L0.7H)^2)/air, and a spectral response in 115–760 nm are embedded. We can see from Figure 4, the reflectance at 121.6 nm is 71%, the bandwidth is 10 nm. Compared with Figure 2, sidelobe ripples in 130.4 nm and 135.6 nm are further suppressed, which will benefit much for imaging detection because there are strong emissions in these two lines. It should be noted that the physical thicknesses of the first and last layers in our multilayers are less than 10 nm, and we corrected those to be 10 nm, which had a negligible effect on the spectral performance.

<Insert Fig. 3>

<Insert Fig. 4>

Minus Filter with a Bandwidth of 5 nm

This section describes further optimization of the above-designed multilayer. In order to achieve a 121.6 nm minus filter with a bandwidth of 5 nm, we utilized OptiLayer software to optimize the above-designed multilayer.[16] As shown in Figure 5, a Gaussian envelop was used to describe the profile of 121.6 nm reflection zone with a bandwidth of 3 nm. The constrained optimization[17] function was employed to optimize the multilayer (Figure 4). The physical thickness limit is from 10 nm to 100 nm. Figure 5 reveals theoretical reflectance curve of multilayer optimized by the constrained optimization function of the OptiLayer software, and the theoretical reflectance curve in 115–760 nm was embedded. We can see from Figure 5, a minus filter with a reflectance of 42.2% and a bandwidth of 5 nm was obtained, but sidelobe ripples of the right side are still significant (<10%), which needed further suppression.

<Insert Fig. 5>

<Insert Fig. 6>

Next, we used the theoretical reflectance curve of the multilayer optimized by constrained optimization to replace the Gaussian type target as a new one of the 121.6 nm reflection zone, while no changes were made in the wavelength range of 130–760 nm. We employed the sensitivity-directed refinement (SDR)[18] function, with the help of the needle optimization technique of the OptiLayer software, to further optimize the multilayer of Figure 5. Figure 6 shows the theoretical reflectance curve of the multilayer optimized using the OptiLayer software SDR, and the theoretical reflectance curve in 115–760 nm was embedded. The physical thickness of each layer in this final design is shown in Figure S4. The thickness error analysis is shown in Figure S5, and the relatively thickness deviation is $\pm$2%. Deviations in the optical performances resulting from thickness error are relatively small, and our final design is easily deposited. As noted in Figure 6, the reflectance at 121.6 nm is 39%, the bandwidth is 5 nm, and the reflectance of sidelobe ripples is less than 5%.

Conclusion

A 121.6 nm minus filter with a bandwidth of 10 nm was designed using the SELs of the matching admittance of multilayers to substrate and air, and equivalent parameters function in Macleod software was utilized to calculate equivalent parameters (admittance and phase

thickness). A 121.6 nm minus filter with a bandwidth of 5 nm was designed using the constrained optimization and SDR functions of OptiLayer software. These two filters all have low sidelobe ripples of 121.6 nm in the reflection zone. This first design provides a good preliminary structure for the optimization of computer software.

Funding

This work is supported by the Joint Research Fund in Astronomy (U1531106) under cooperative agreement between the National Natural Science Foundation of China (NSFC) and Chinese Academy of Science (CAS), partially supported by NSFC (Grant No.11427803), and partially supported by the Strategic Priority Research Program of Chinese Academy of Science (CAS), Grant No. XDA15320103.

Supplemental Material

All supplemental material mentioned in the text, consisting of Figures S1 to S5, is available in the online version of the journal.

References

1. B. Li, H. Li, S. Zhou, B. Jiang. "The Lyman-Alpha Imager Onboard Solar Polar Orbit Telescope". Proc. of SPIE 2013. 9042: 90420Y.
2. N. Narukage, D.E. Mckenzie, R. Ishikawa, J.T. Bueno, et al. "Chromospheric Layer Spectropolarimeter (CLASP2)". Proc. of SPIE 2016. 9905: 990508.
3. R. Kano, T. Bando, N. Narukage, R. Ishikawa, et al. "Chromospheric Lyman-Alpha Spectro-Polarimeter (CLASP)". Proc. of SPIE 2012. 8443: 84434F.
4. E.A. West, J G. Porter, J.M. Davis, G.A. Gary, et al. "The Marshall Space Flight Center Solar Ultraviolet Magnetograph". Proc. of SPIE 2004. 5488: 801.
5. W.A. Podgorski, P.N. Cheimets, L. Golub, J.R. Lemen, et al. "Design, Performance Prediction, and Measurements of the Interface Region Imaging Spectrograph (IRIS) Telescope". Proc. of SPIE 2012. 8443: 84433D.
6. L.R. Marcos, J.I. Larruquert, J.A. Méndez, J.A. Aznárez. "Multilayers and Optical Constants of Various Fluorides In the Far UV". Proc. of SPIE 2015. 9627: 96270B.

7. R.B. Hoover, T.W. Barbee, J.P.C. Baker, J.F. Lindblom, et al. “Performance of Compact Multilayer Coated Telescopes at Soft X-Ray/EUV and Far Ultraviolet Wavelengths”. Opt. Eng. 1990. 29(10): 281–290.
8. J.H. Park, M. Zukic, M. Wilson, C.E. Keffer, et al. “Design and Fabrication of Multilayer Reflective Filters for a Ritchey–Chretien Lyman-A Telescope”. Opt. Eng. 1996. 35(5): 1479–1482.
9 N. Narukage, M. Kubo, R. Ishikawa, S. Ishikawa, et al. “High-Reflectivity Coatings for a Vacuum Ultraviolet Spectropolarimeter”. Solar Phys. 2017. 292(3): 40.
10. X. Wang, B. Chen. “Design of Second-Order 121.6 nm Narrowband Minus Filters Using Asymmetrically Apodized Thickness Modulation”. Appl. Phys. B: Lasers Opt, paper submitted.
11. X. Wang, B. Chen. “Design of Dual Band Cold Mirrors”. Sci. Rep. 2017. 7: 15402.
12. H.A. Macleod. Macleod Software. http://www.thinfilmcenter.com [accessed 6 April 2018].
13. M.-C. Liu, C.-C. Lee, M. Kaneko, K. Nakahira, et al. “Microstructure-Related Properties at 193 nm of MgF_2 and GdD_3 Films Deposited by a Resistive-Heating Boat”. Appl. Opt. 2006. 45(7): 1368–1374.
14. H.A. Macleod. Thin-Film Optical Filters, 4th ed. (CRC Press, 2010).
15. A. Thelen. “Equivalent Layers in Multilayer Filters”. J. Opt. Soc. Am. 1966. 56: 1533-1538.
16. A.V. Tikhonravov, M.K. Trubetskov. OptiLayer Thin Film Software. http://www.optilayer.com [accessed 6 April 2018].
17. A.V. Tikhonravov, M.K. Trubetskov, T.V. Amotchkina. “Application of Constrained Optimization to the Design of Quasi-Rugate Optical Coatings”. Appl. Opt. 2008. 47(28): 5103–5109.
18. T. Amotchkina, U. Brauneck, A. Tikhonravov, M. Trubetskov. “Sensitivity-Directed Refinement for Designing Broadband Blocking Filters”. Opt. Express 2015. 23(5): 5565–5570.

Captions

Figure 1. Theoretical reflectance curves of modified multilayer ((0.7H0.6L0.7H)^11 mH), and the incidence angle is 10°.

10.1177/0003702818788828

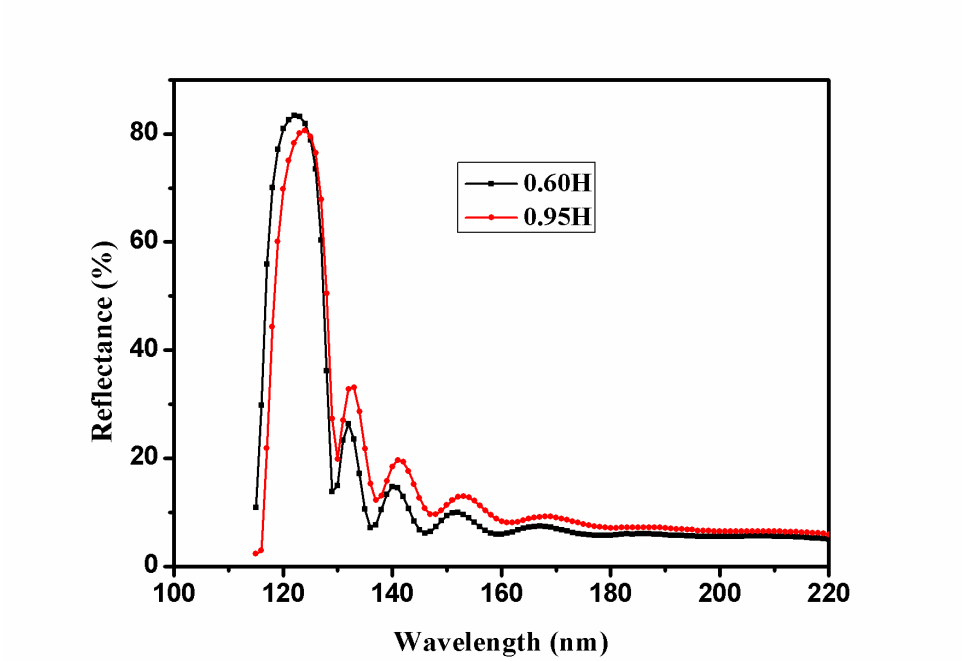

Figure 2. Theoretical reflectance curve of multilayer with a structure of sub/((0.7H0.6L0.7H)^9 0.6H0.964(0.7H0.6L0.7H)^2)/air, and the incidence angle is 10°.

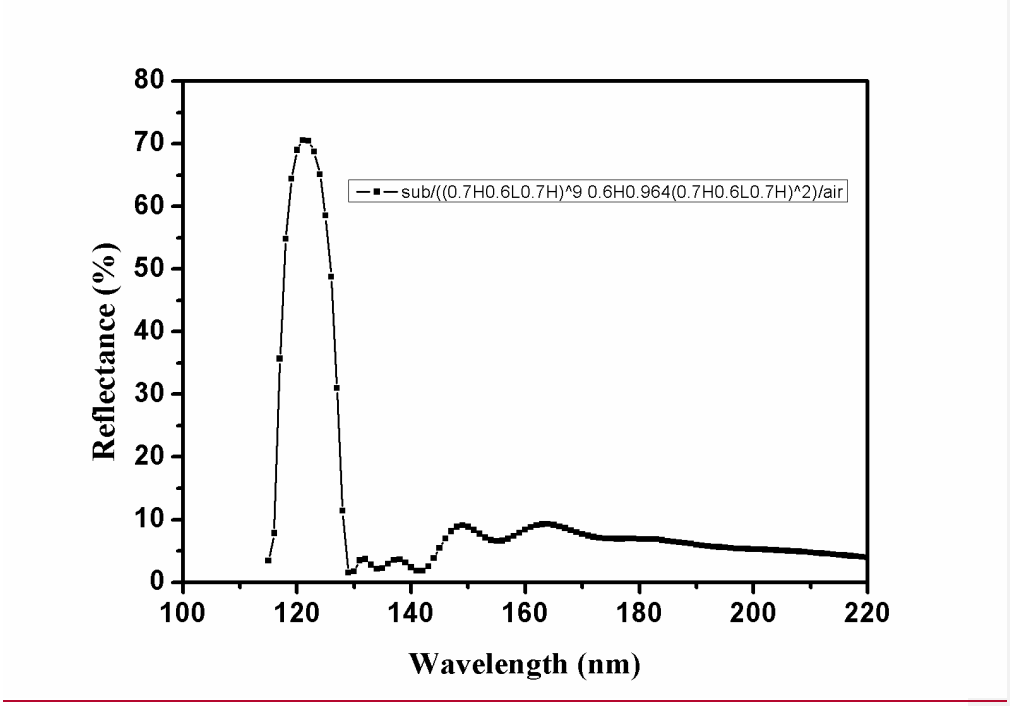

Figure 3. Real pat of equivalent admittance of multilayer 0.9(0.7H0.6L0.7H), the incidence angle is 10°.

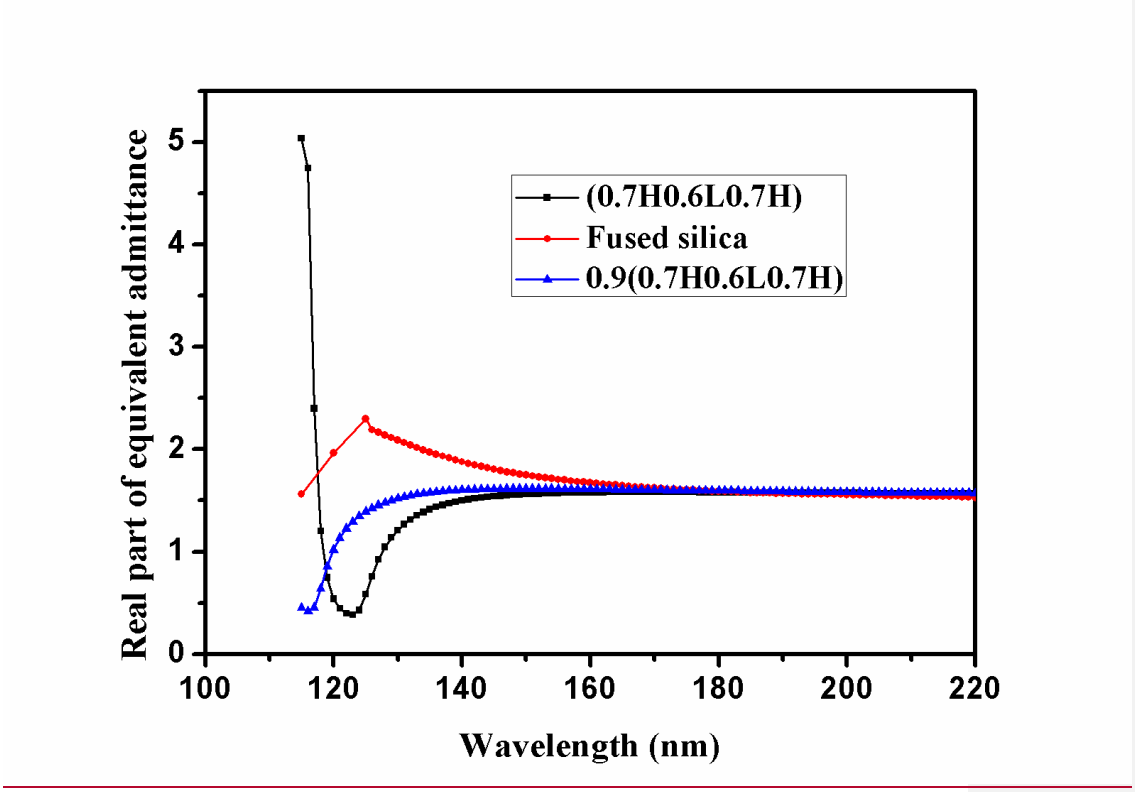

Figure 4. Theoretical reflectance curve of multilayer with a structure of sub/(0.9(0.7H0.6L0.7H)^2 (0.7H0.6L0.7H)^7 0.6H0.964(0.7H0.6L0.7H)^2)/air, and the incidence angle is 10°.

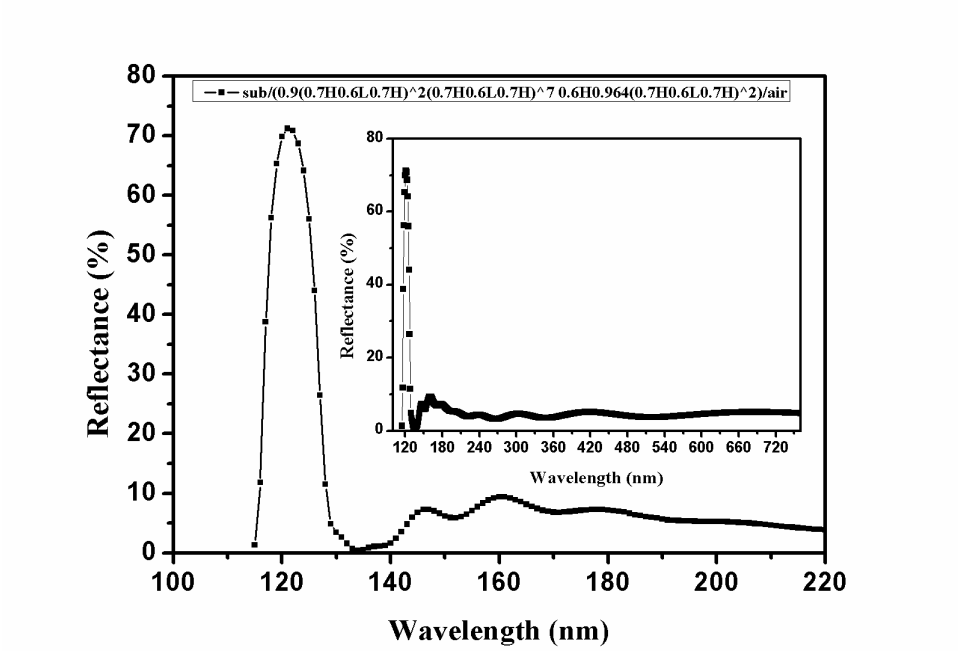

Figure 5. Theoretical reflectance curve of multilayer optimized by Constrained Optimization of OptiLayer software, and the incidence angle is 10°.

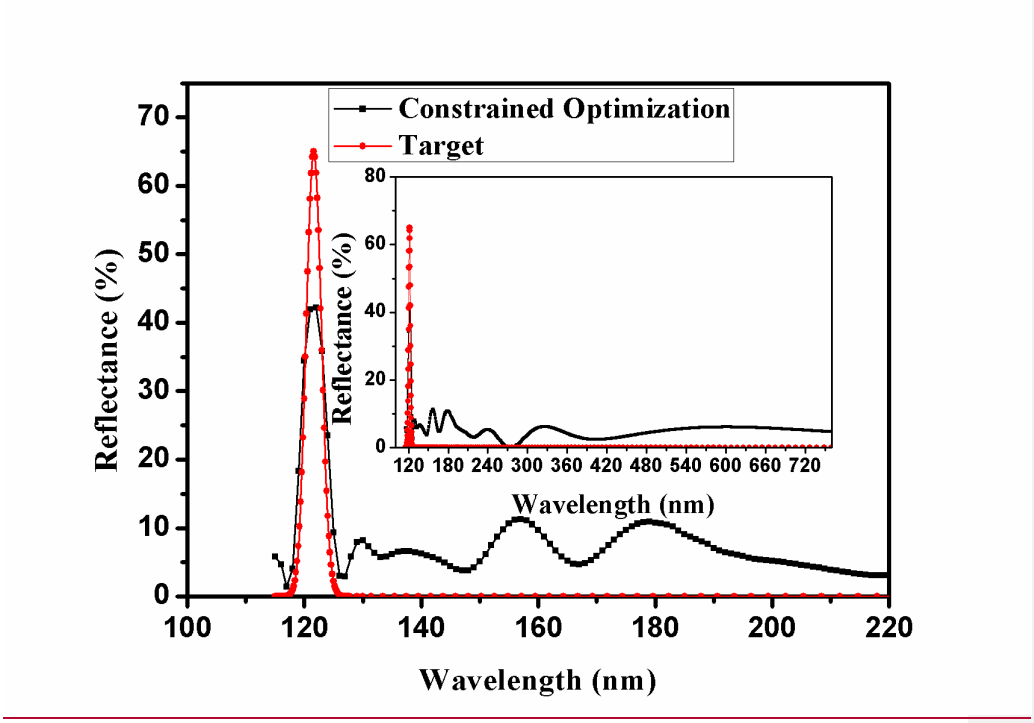

Figure 6. Theoretical reflectance curve of multilayer optimized using SDR of OptiLayer software.

10.1177/0003702818788828

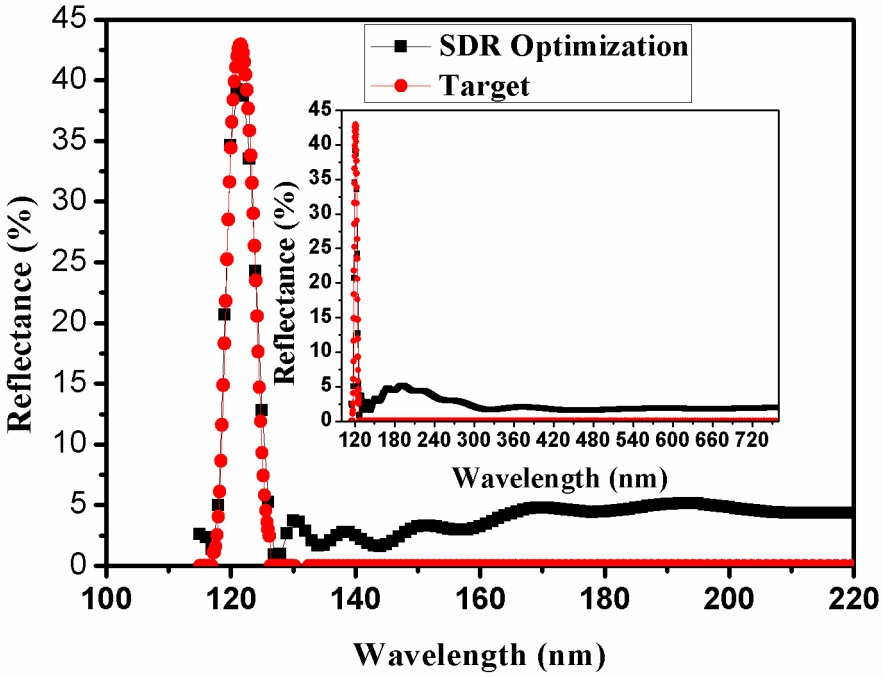

Formatted: Space After: 10 pt, Line spacing: Multiple 1.15 li, Tab stops: Not at 0.5"

Supplemental Material

Design of First-Order 121.6 nm Minus Filters

Xiaodong Wang*[,1], Bo Chen[1], Tonglin Huo[2], Hongjun Zhou[2]

10.1177/0003702818788828

1. State Key Laboratory of Applied Optics, Changchun Institute of Optics, Fine Mechanics and Physics, Chinese Academy of Sciences, Changchun 130033, China

2. National Synchrotron Radiation Laboratory, University of Science and Technology of China, Hefei 230026, China

Corresponding author email: wangxiaodong@ciomp.ac.cn

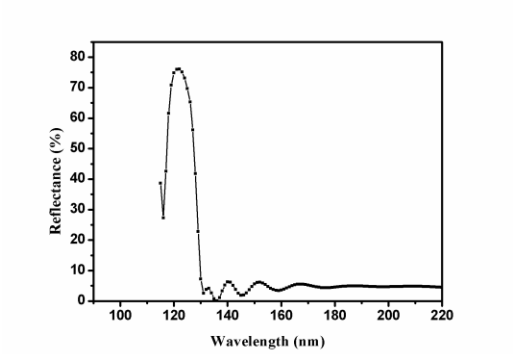

Figure S1. Theoretical reflectance curve of periodic multilayer of sub/(0.7H0.6L0.7H)^11/air, and the incident angle is 10°.

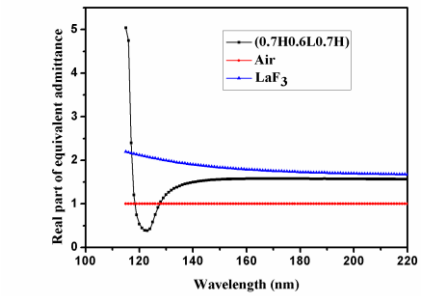

10.1177/0003702818788828

Figure S2. Real part of equivalent admittance of periodic multilayer (0.7H0.6L0.7H), and the incidence angle is 10°.

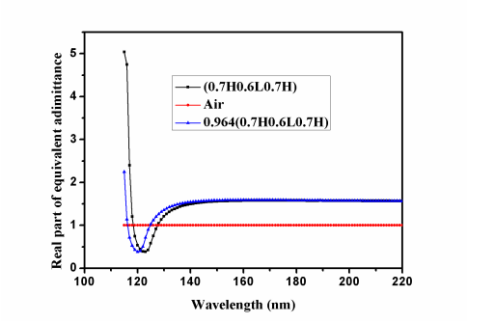

Figure S3. Real pat of equivalent admittance of multilayer 0.964(0.7H0.6L0.7H), the incidence angle is 10°.

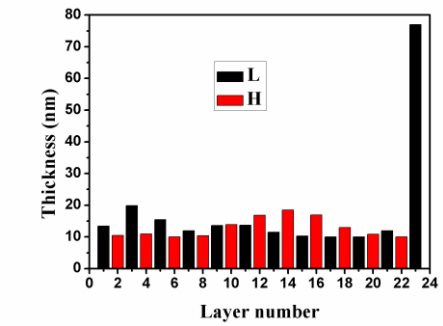

Figure S4. Final design result of 121.6 nm minus filter.

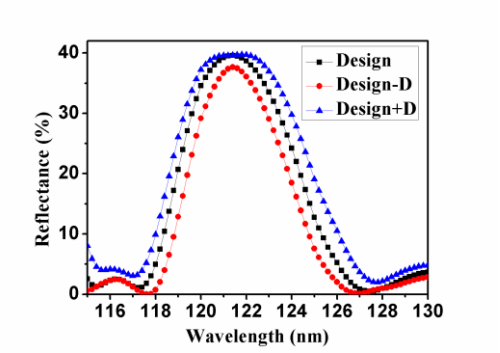

Figure S5. Error analysis result of final design.

Formatted: Space After: 10 pt, Line spacing: Multiple 1.15 li, Tab stops: 4.36", Left + Not at 0.5"